XL CILAMCE
IBERO-LATIN AMERICAN CONGRESS ON COMPUTATIONAL METHODS IN ENGINEERING
NOVEMBER 11-14, 2019
Praiamar Natal Hotel & Convention
Natal, RN-BRAZIL

STRUCTURAL OPTIMIZATION OF TRUSSES UNDER ELASTIC AND INELASTIC BUCKLING CONSTRAINTS

Marcela A. Juliani
Mariana O. Milanez
Wellison J. S. Gomes
marcelajulianii@gmail.com
mariana.omilanez@gmail.com
wellison.gomes@ufsc.br
Center for Optimization and Reliability in Engineering (CORE), Department of Civil Engineering, Federal University of Santa Catarina.
João Pio Duarte da Silva S., 88037-000, Santa Catarina, Brazil

Abstract. It is well known in the literature and practice of structural optimization that optimal structural configurations are highly dependent on the constraints applied to the problem or, in other words, on the definition of what is feasible or not. Results obtained under a certain type of constraints may be not optimal, or even not acceptable, if other types of constraints are considered. Discussions related to constraints and their effects on structural optimization are found in many papers, but only a few of them directly address this subject. In the specific case of optimization of trusses, it is common to find applications involving two different scenarios, where stress-based constraints are combined with elastic buckling or with inelastic buckling constraints, respectively. The first scenario is much more common, and the differences between results related to each of these combinations are hardly ever discussed or emphasized. The present paper focus on the comparison of structural optimization of trusses, considering these two scenarios, in an attempt to identify in which cases similar results are obtained and how different the results can be. The paper also proposes a simple multistart optimization scheme combined with sequential quadratic programming, so that the optimization problems are solved in a global and efficient manner, and the comparisons are not significantly compromised by local minima. Two trusses are evaluated, for some different cases of boundary conditions, and the results indicate that the optimal configurations may be significantly different in the cases where a sufficient number of compressed slender bars is present.

Keywords: Structural optimization, Trusses, Elastic buckling, Inelastic buckling, Multistart optimization

1 Introduction

Among the areas of research related to structural engineering, there is a wide field of studies related to structural optimization. In this context, many papers have been published in recent years, in order to find structures which are optimal with respect to the functions they fulfill and respect the imposed constraints (Luh and Lin [1], Stromberg et al. [2], Camp and Huq [3], Miguel et al. [4], Zegard and Paulino [5], Farshchin et al. [6], Tapao and Cheerarot [7], Gomes et al. [8], Tejani et al. [9]).

Usually, optimal structural configurations are highly dependent on the natural and essential boundary conditions considered, as well as on the mathematical/numerical models employed to represent the structural behavior. There are some studies in the literature that discuss such aspects of optimization: Pezeshk et al. [10], Suleman and Sedaghati [11] and Lanes et al. [12] analyze the effect of the structural model on the optimal structural configuration; Buhl et al. [13], Jung and Gea [14], Kemmler et al. [15], Klarbring and Strömberg [16] and Zhang et al. [17] present and discuss optimal results obtained by considering different structural models, prescribed loads and displacements.

It is known from the literature that, in optimization problems, the constraints define which design solutions are feasible or not (Nocedal and Wright [18], Arora [19]). Thus, the optimal configuration of a structure, obtained under a certain type of constraints, may be not optimal, or even unfeasible, if another type of constraints is considered. The effect of constraints on the structural optimization response has been addressed in some papers, but few of them discuss this subject directly (Torii et al. [20], Juliani and Gomes [21, 22], Petrović et al. [23]).

In the specific case of optimization of trusses, it is common to find applications involving two different scenarios, where stress-based constraints are combined with elastic buckling or with inelastic buckling constraints, respectively (Tejani et al. [9], Torii et al. [20], Galante [24], Guo et al. [25], Pedersen and Nielsen [26], Guo et al. [27], Mela [28]). Although the second scenario usually leads to a better representation of the structural behavior, the first scenario is much more common due to the simplicity and to the lower computational cost associated. However, the differences between optimization results related to each of these combinations are hardly ever discussed or emphasized.

The present paper proposes to analyze the optimal configuration of plane trusses, through the minimization of the volume of the structural elements, considering two distinct scenarios of constraints: scenario 1 considers elastic buckling constraints, characterized by Euler buckling stress; scenario 2 considers inelastic buckling constraints, represented by a single stability criterion. In both cases, constraints related to yielding of the bars are also considered. Two numerical examples from the literature are evaluated: a two-bar truss (Beck and Gomes [29]) and a five-bar truss (Aoues and Chateauneuf [30]). The first example is studied for 9 different cases, related to distinct directions of the applied load, and the second example is studied for 2 different cases, related to distinct supports of the structure. Such studies are conducted to identify in which cases similar results are obtained for both scenarios and how different the results can be. The paper also proposes a simple multistart optimization scheme combined with sequential quadratic programming (SQP), so that the optimization problems are solved in a global and efficient manner, and the comparisons are not significantly compromised by local minima.

The remainder of this paper is organized as follows: section 2 presents the formulation of the structural optimization problem that is addressed in this paper; the multistart optimization method, which is combined with sequential quadratic programming, is described in section 3; section 4 presents the application of the proposed approach to two numerical examples; conclusions and discussions about the results obtained in this paper are presented in section 5.

2 Structural optimization formulation

A constrained optimization problem can be described according to Eq. 1, where the vector of design variables is represented by $\mathbf{x}$, which contains the n variables, x_i, of the problem, with $i = 1, ..., n$; $f(\mathbf{x})$ is the objective function; $\mathbf{g}$ is the vector of constraints, where m is the number of constraint functions $g_i(\mathbf{x})$, with $i = 1, ..., m$.

$$\begin{aligned} &\text{- Find } \mathbf{x} = (x_1, ..., x_n); \\ &\text{- That minimize } f(\mathbf{x}); \\ &\text{- Subject to } \mathbf{g} = (g_1(\mathbf{x}), ..., g_m(\mathbf{x})) \leq 0. \end{aligned} \tag{1}$$

In the present paper, the dimensions of the cross sections of the bars or their respective areas are taken as design variables, and the objective function is the volume of the structure. Constraints have been divided into two scenarios, and the main difference between these scenarios is the way that buckling is taken into account. In the following sections, the formulations of each scenario are described. It is noteworthy that all calculation routines employed herein were developed in MATLAB (MathWorks [31]), and that the software MASTAN2 (Ziemian and McGuire [32]) was used for structural analysis. The fact that MASTAN2 is also implemented in MATLAB allows for a better coupling between optimization and structural analysis, helping to reduce computational costs.

2.1 Elastic buckling constraints: scenario 1

Elastic buckling is taken into account considering the Euler buckling stress σ_{cr}, calculated according to Eq. 2,

$$\sigma_{cr}(\mathbf{x}) = \frac{\pi^2 EI}{AL_f^2}, \tag{2}$$

where E is the modulus of elasticity of the material, I and A are, respectively, the moment of inertia and the cross-sectional area of the structural element and L_f is the buckling length, taken equal to the length of the bar in the case of trusses. Thus, in this scenario, a first-order elastic analysis of the truss is performed, and then for each one of the n_{bar} bars, the following checks are made (Eq. 3): if the $i\text{-}th$ structural element is under compression, the absolute value of its stress $|\sigma_i(\mathbf{x})|$ must not exceed the lowest stress between the yield stress σ_y and the Euler buckling stress $\sigma_{cr_i}(\mathbf{x})$; if the $i\text{-}th$ structural element is under tension, its stress $\sigma_i(\mathbf{x})$ must not exceed σ_y.

$$\underset{(i=1,...,n_{bar})}{g_i(\mathbf{x}) =} \begin{cases} \dfrac{|\sigma_i(\mathbf{x})|}{\min(\sigma_y, \sigma_{cr_i}(\mathbf{x}))} - 1 \leq 0, & \text{if } \sigma_i(\mathbf{x}) < 0; \\ \dfrac{\sigma_i(\mathbf{x})}{\sigma_y} - 1 \leq 0, & \text{if } \sigma_i(\mathbf{x}) > 0. \end{cases} \tag{3}$$

2.2 Inelastic buckling constraints: scenario 2

In this scenario, a single constraint is considered, given by Eq. 4,

$$g(\mathbf{x}) = \frac{P}{P_{cr}(\mathbf{x})} - 1 \leq 0, \tag{4}$$

where P is the applied load and $P_{cr}(\mathbf{x})$ is the critical load, which is the maximum load value that the structure can handle before reaching failure. In this scenario, failure may occur due to buckling or

yielding of one or more bars. In order to incorporate the possibility of buckling and yielding in the computation of the critical load, it is necessary to impose initial imperfections to each bar of the structure and to perform inelastic and geometrically nonlinear structural analyses. To do so, in this paper the initial imperfections are based on some of the first vibration modes of the structure and the materials are assumed to have elastic-perfectly plastic characteristics.

Therefore, in this scenario, the following procedure is carried out: first, an eigenvalue analysis of the structure is performed; then, for each vibration mode considered, the critical load is calculated by second-order inelastic analysis, taking into account a perturbation in the nodal coordinates of the structure, according to Eq. 5; finally, Eq. 4 is checked for each one of the critical loads evaluated.

$$\mathbf{c} = \mathbf{c}_0 + 0.001\mathbf{u}. \tag{5}$$

Where:

$\mathbf{c}$ = Vector of nodal coordinates after perturbation;

$\mathbf{c}_0$ = Vector of inicial nodal coordinates;

$\mathbf{u}$ = Vector of nodal displacements, according the vibration mode considered in the eigenvalue analysis.

In structural analysis, truss bars are modeled using several frame elements with moment releases at hinged connections. So, elements that are connected to hinges are modeled as fixed-hinge frame element while others are modeled as fixed-fixed elements. For more details about the model the readers are referred to Madah and Amir [33], since the structural model adopted herein is very similar to the ones described in this paper.

Figure 1 shows the critical load obtained for a column previously studied by McGuire et al. [34]. The imperfection applied was a displacement in the nodes, proportional to the length of the column (Fig. 1(a)). It can be seen that after P_{cr} the structure loses its strength abruptly (Fig. 1(b)).

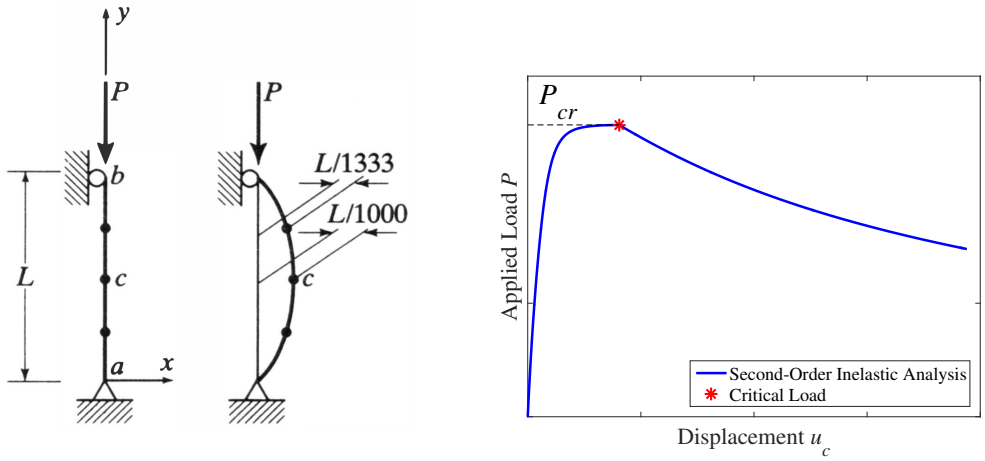

(a) Structure and its perturbation (McGuire et al. [34]).

(b) Analysis performed using the software MASTAN2.

Figure 1. Hinged end column.

3 Multistart optimization

Search methods based on local optimization that aims at finding global optimal solutions need some way of diversification to overcome local optimality. If this diversification is not applied, such methods can explore only a small region of the domain and are not able to find global optimal solutions. Thus,

many strategies have been studied to overcome this problem, one of them is called multistart. In this method, diversification is applied by restarting the search from a new point in the domain once a region has been widely explored (Martí [35]).

This paper proposes a multistart optimization scheme combined with sequential quadratic programming (SQP). The proposed multistart method is based on the distance between points in a sample of the design domain. Thus, after a region has been explored by SQP, starting from a selected point in the sample, the next starting point is defined as the farthest apart point from the ones already selected. Thus, it is intended to explore the domain as a whole, including the most and least promising regions, trying to escape from possible local minima. The SQP used in this paper is available in MATLAB by means of the fmincon function, and more details about it may be obtained from Nocedal and Wright [18].

Figure 2 presents the pseudo-code of the method, which can be summarized as follows: initially, a sample of the design domain is generated, consisting of (N_{samp}-1) random points and 1 feasible point defined by designer ($\mathbf{x}_1$); then SQP is applied, taking $\mathbf{x}_1$ as a starting point, and resulting in an optimal design vector $\mathbf{x}^*$, which is the best result found until the moment ($\mathbf{x}^{best}$); multistart is initiated, selecting a next point from the sample with maximum distance to the points already selected; if this point meets the constraints, it is used as a starting point for a new SQP search, finding a new value of $\mathbf{x}^*$; if $f(\mathbf{x}^*)$ is less than $f(\mathbf{x}^{best})$, the value of $\mathbf{x}^{best}$ is updated to the value of $\mathbf{x}^*$; multistart runs until some stopping criterion is met. In this paper, the algorithm is stopped if the number of points selected reaches a predefined value N_{ED} or the number of feasible points reaches a maximum value of N_{max}.

Figure 3 illustrates how the domain of an optimization problem was explored by the method. The arrows indicate the order of selection of the points. For this case, the following parameters and initial point were used: $N_{samp} = 50$, $N_{ED} = 15$, $N_{max} = 5$ and $\mathbf{x}_1 = (5, 150)$.

begin

Define the problem: $\mathbf{x}$, $f(\mathbf{x})$ and $\mathbf{g}$

Define input data: N_{samp}, N_{ED} e N_{max}

Generate random sample $\mathbf{x}_i$ $(i = 2, ..., N_{samp})$ and define a feasible $\mathbf{x}_1$

Apply SQP with $\mathbf{x}_1$ as starting point: find $\mathbf{x}^*$

Do $\mathbf{x}^{best} = \mathbf{x}^*$, $j = 1$ and $k = 1$

while $j < N_{ED}$ and $k < N_{max}$

    Do $j = j + 1$

    Select from sample the farthest apart point $\mathbf{x}_{far}$ from those already selected

    if $\mathbf{x}_{far}$ is feasible

        Do $k = k + 1$

        Apply SQP with $\mathbf{x}_{far}$ as starting point: find a new $\mathbf{x}^*$

        if $f(\mathbf{x}^*) < f(\mathbf{x}^{best})$

            Do $\mathbf{x}^{best} = \mathbf{x}^*$

        end if

    end if

end while

Postprocess results and visualization

end begin

Figure 2. Pseudo-code of the multistart optimization scheme combined with SQP.

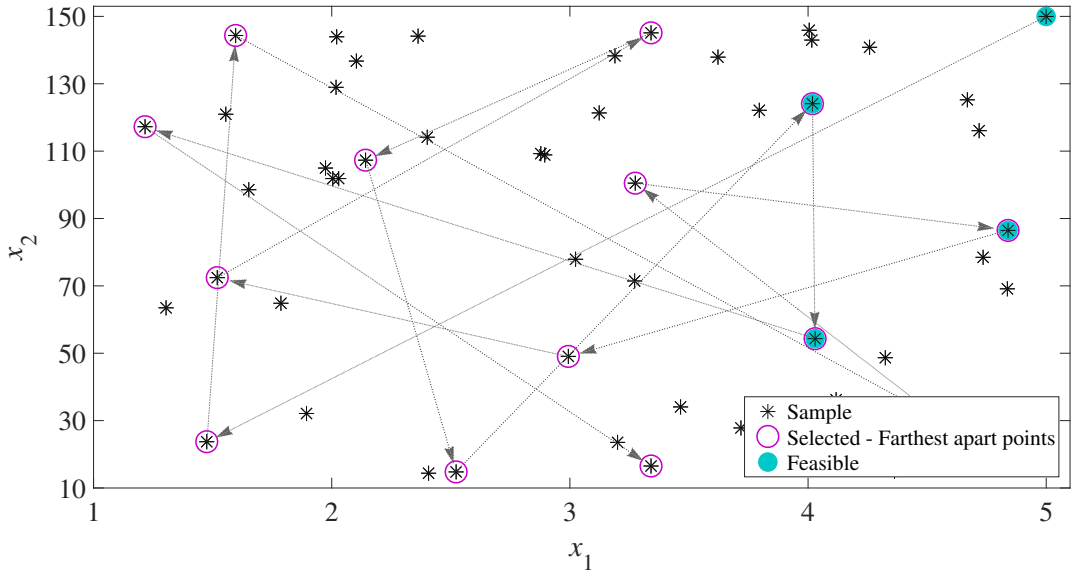

Figure 3. Exploration of the domain.

4 Numerical examples

In order to inquire the differences between the optimal configurations of the structures for each constraints scenario, two numerical examples are evaluated, each one related to a given truss obtained from the literature. The multistart parameters used for both examples are: $N_{samp} = 10^6$, $N_{ED} = 4000$ and $N_{max} = 20$.

4.1 Two-bar plane truss

The first example is a two-bar plane truss, studied by Beck and Gomes [29], and presented in Fig. 4(a). The span $2B$ is fixed and the optimization variables are the height H of the truss, mean diameter d and tube thickeness t of bar (1) and bar (2), that is, $\mathbf{x} = (H, d_1, t_1, d_2, t_2)$. The structure is optimized for 9 different directions of the applied load P (Fig. 4(b)). For cases where $\theta \geq 120^{\text{o}}$, only the first-order inelastic analysis is considered in scenario 2, since for these angles no buckling occurs. In these cases the only failure mode applicable for the structure is the one related to yielding of one or more bars. In addition to the constraints of each scenario, a limitation to the ratio d/t of each bar is also imposed: this ratio must be greater than 2, so that the thickness is not larger than half the diameter, and less than 10, to avoid local instability of tube walls. It is noteworthy that the approximation $A = \pi dt$ is used to compute the cross-sectional area, and that in scenario 2 only the first two vibration modes are considered. Table 1 shows the input data for this example.

Table 2 presents the optimal results for each scenario and load case, and, for illustrative purposes, Fig. 5 shows the optimal configurations for $\theta \leq 90^{\text{o}}$. It is emphasized that all results met a minimum constraints tolerance of 10^{-8}, except for $\theta = 135^{\text{o}}$ and $\theta = 150^{\text{o}}$ from scenario 2, where the violation was approximately 10^{-3}.

It is worth noting that $d/t = 10$ was observed for all compressed bars in both scenarios. This indicates that it is more useful for elements subject to buckling, that the cross sections have larger diameters and thinner thickness than the opposite, since for a given area the moment of inertia is higher in the first case. For bars under tension, this fact was not observed in most cases, since inertia is not as influential in the result. This difference in the ratio d/t for compressed and tensioned bars can be clearly seen at $\theta = 90^{\text{o}}$ in both scenarios, where for bar (1) $d_1/t_1 = 8.8$ and for bar (2) $d_2/t_2 = 10$.

Note in Fig. 6 that the difference between the volume of the optimal structures for each scenario

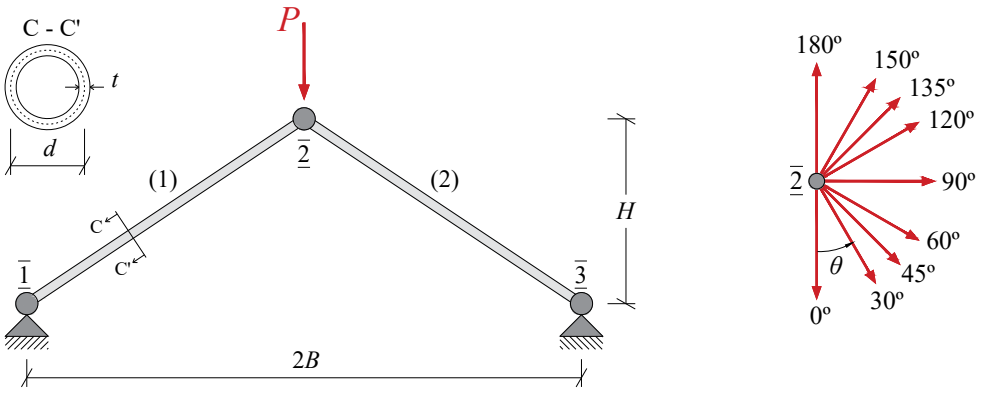

(a) Original problem. (b) Load cases.

Figure 4. Two-bar truss problem.

Table 1. Input data for the two-bar truss problem.

Data	Value
Load P	674 kN
Elastic modulus E	30 GPa
Yield stress σ_y	105 MPa
Lower bounds of the design variables $\mathbf{x}_l$	(1.5, 0.1, 0.01, 0.1, 0.01) m
Upper bounds of the design variables $\mathbf{x}_u$	(2, 0.2, 0.02, 0.2, 0.02) m
Starting point $\mathbf{x}_1$	(2, 0.2, 0.02, 0.2, 0.02) m

is larger for $\theta = 0^{\text{o}}$, where both bars are equally compressed, and decreases for increasing values of θ up to $\theta = 90^{\text{o}}$, where bar (1) is under tension stress. For these load cases, scenario 2 leads to a higher volume than scenario 1. For $\theta > 90^{\text{o}}$, the difference found between the volume of the optimal structures for each scenario very small, and the values of the objective function can be considered equal for each θ. Therefore, this shows that scenario 2 is more restrictive than scenario 1 for elements under compression, and both tend to be equivalent for elements under tension. It is noteworthy that the volume of the structure, in both scenarios, decreases in the interval from $\theta = 0^{\text{o}}$ to $\theta = 90^{\text{o}}$ and, after this angle, the volume increases when θ is increased up to 180^{o}; however, for most cases, the volumes are larger for angles below 90^{o} than for angles greater than 90^{o}. This shows that compressed elements require more robust structures than tensioned elements to meet loads of equal magnitude.

Fig. 7 shows that the highest difference between the optimal cross-sectional areas of the elements for each scenario occurred in bar (2), for θ between 30^{o} and 60^{o}. For such angles, this bar tends to be under higher compression forces, indicating that the more compressed the element, the greater the differences between the optimal configuration of each scenario, as expected, and the more restrictive the scenario 2. For the other load cases, the difference between the optimal areas of each scenario was small, although the values of d and t are not the same.

In order to verify the quality of the optimal results obtained, the convergence curve of the SQP algorithm for the initialization of the multistart that resulted in the optimal solution is presented in Fig. 8. It can be seen that the algorithm stopped after converging to a result, not by iteration limitations. Thus, the differences found between the optimal points for each scenario and load case are less sensitive to be of poor performance of the optimization method.

Table 2. Optimization results for the two-bar truss problem.

Scenario 1						
θ (°)	$f(\mathbf{x})$ (m^3)	H (m)	d_1 (m)	t_1 (m)	d_2 (m)	t_2 (m)
0	0.0566	1.5000	0.1639	0.0164	0.1639	0.0164
30	0.0521	1.5442	0.1444	0.0144	0.1683	0.0168
45	0.0458	1.6978	0.1207	0.0121	0.1664	0.0166
60	0.0379	1.5000	0.1000	0.0100	0.1611	0.0161
90	0.0321	1.5000	0.1000	0.0114	0.1378	0.0138
120	0.0330	1.5590	0.1451	0.0145	0.1000	0.0100
135	0.0357	1.7675	0.1504	0.0150	0.1000	0.0100
150	0.0363	1.9711	0.1486	0.0150	0.1000	0.0100
180	0.0417	2.0000	0.1252	0.0147	0.1264	0.0146
Scenario 2						
θ (°)	$f(\mathbf{x})$ (m^3)	H (m)	d_1 (m)	t_1 (m)	d_2 (m)	t_2 (m)
0	0.0626	1.9320	0.1671	0.0167	0.1671	0.0167
30	0.0570	1.8690	0.1405	0.0140	0.1777	0.0178
45	0.0494	2.0000	0.1131	0.0113	0.1756	0.0176
60	0.0413	1.5000	0.1000	0.0100	0.1709	0.0171
90	0.0325	1.5000	0.1000	0.0115	0.1392	0.0139
120	0.0330	1.5580	0.1403	0.0150	0.1000	0.0100
135	0.0356	1.6941	0.1250	0.0183	0.1000	0.0100
150	0.0362	1.9711	0.1262	0.0175	0.1000	0.0100
180	0.0417	2.0000	0.1214	0.0152	0.1297	0.0142

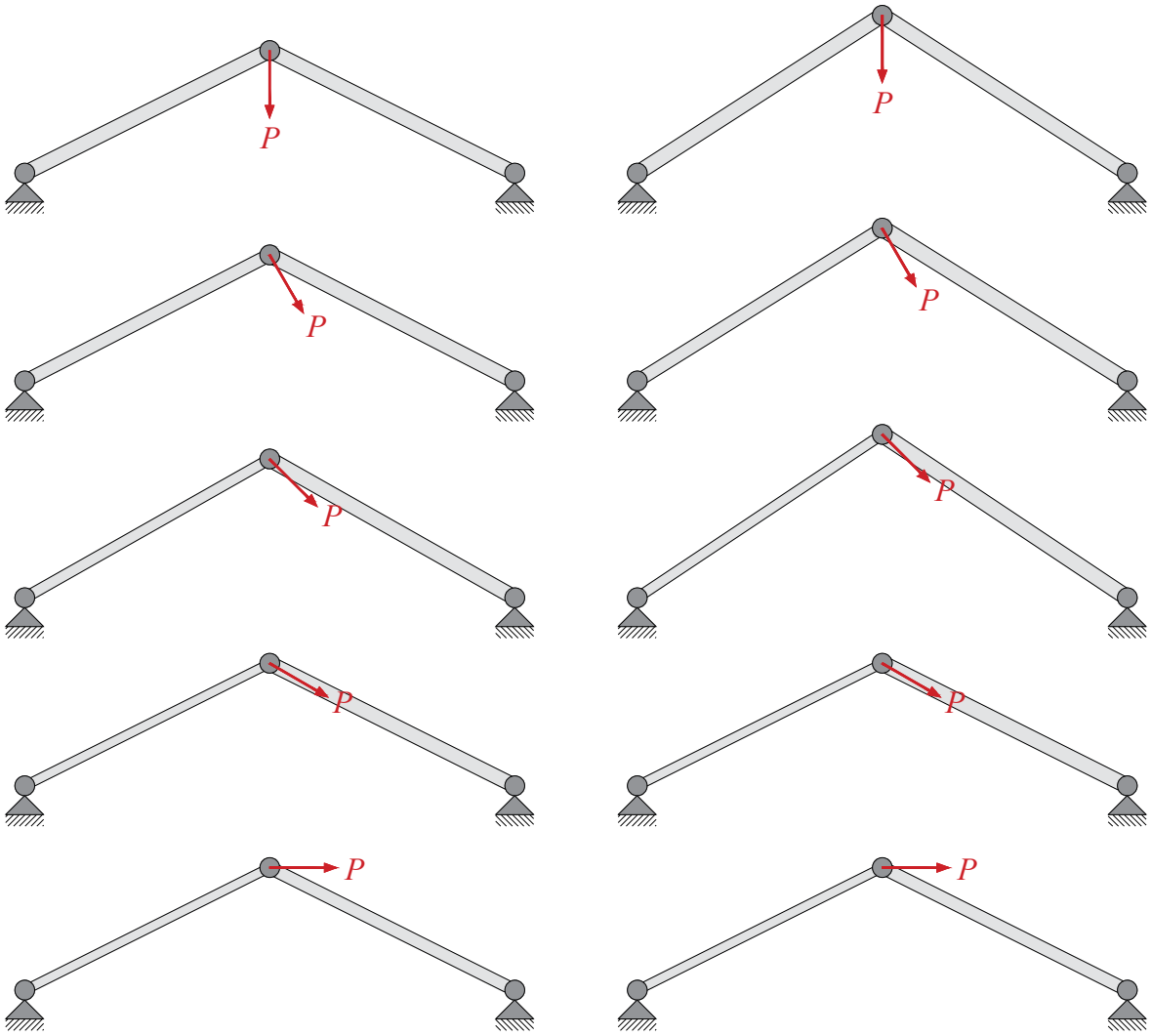

(a) Scenario 1. (b) Scenario 2.

Figure 5. Optimal configurations for $\theta = 0^{o}$ to 90^{o}.

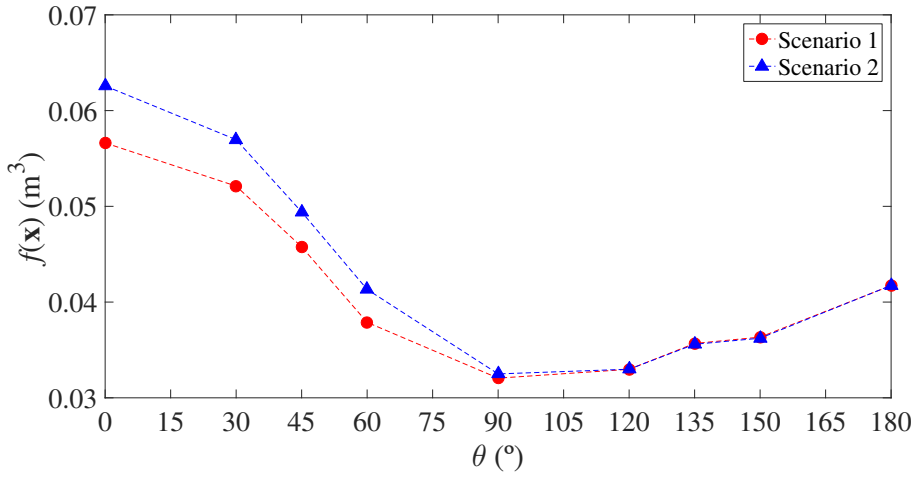

Figure 6. Relation between direction of the load and optimum volume.

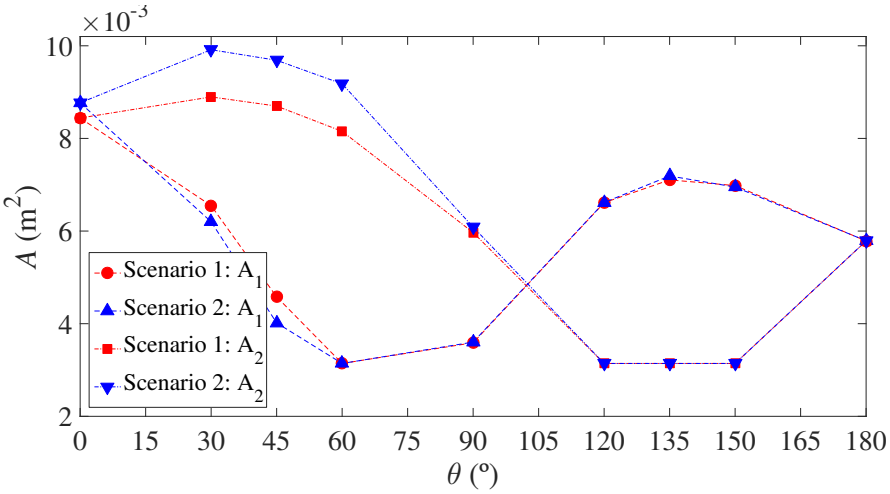

Figure 7. Relation between direction of the load and optimum cross-sectional area.

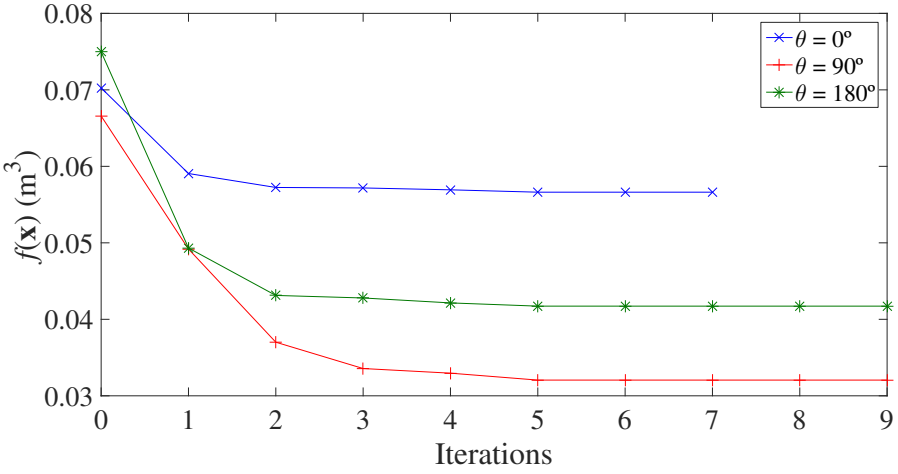

(a) Scenario 1.

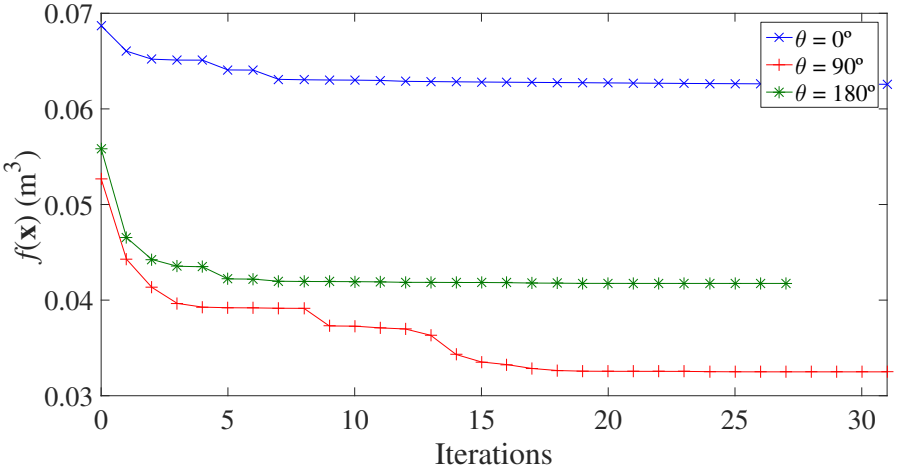

(b) Scenario 2.

Figure 8. Convergence of SQP algorithm.

4.2 Five-bar plane truss

The second example is a five-bar plane truss, studied by Aoues and Chateauneuf [30], and presented in Fig. 9(a). The span and height are fixed and the variables are the cross-sectional areas of each bar, hence, $\mathbf{x} = (A_1, A_2, A_3, A_4, A_5)$. In addition to the original truss, the structure is optimized for a different boundary condition, in which the support of node 4 is modified (Fig. 9(b)). All bars are considered to have circular cross sections, and, in scenario 2, three vibration modes are taken into account. Table 3 summarizes the input data for this example.

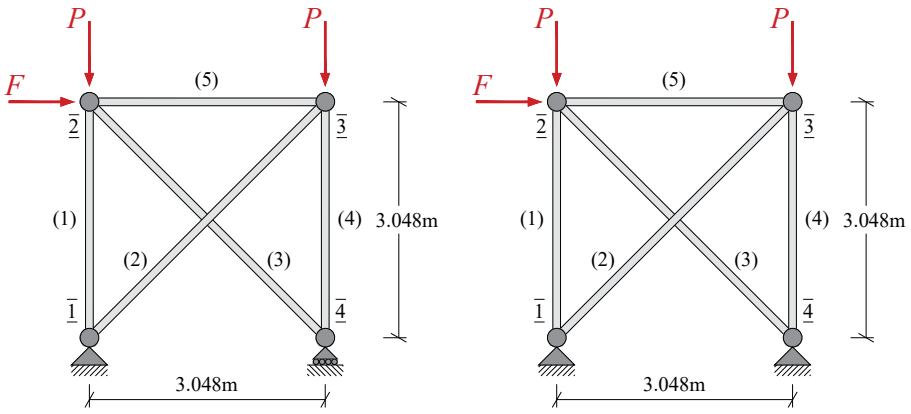

(a) Original. (b) Modified.

Figure 9. Five-bar truss problem.

Table 3. Input data for the five-bar truss problem.

Data	Value
Load P	15 kN
Load F	20 kN
Elastic modulus E	68.95 GPa
Yield stress σ_y	172 MPa
Lower bounds of the design variables $\mathbf{x}_l$	(0.7854, 0.7854, 0.7854, 0.7854, 0.7854) $\cdot 10^{-4}$m^2
Upper bounds of the design variables $\mathbf{x}_u$	(78.54, 78.54, 78.54, 78.54, 78.54) $\cdot 10^{-4}$m^2
Starting point $\mathbf{x}_1$	(25, 25, 25, 25, 25) $\cdot 10^{-4}$m^2

Table 4 shows the optimization result for the original problem. Note that the optimal designs are similar, resulting in two structures with the same volume, due to the fact that the structure does not exceed its elastic limit.

Thus, the second case, where the boundary condition is modified, is analyzed only for scenario 1. The optimal design vector for scenario 1 of the modified structure was $\mathbf{x} = (1.0061, 0.7854, 30.2067, 16.6688, 4.5292) \cdot 10^{-4}$ m^2, and $f(\mathbf{x}) = 0.0201$ (m^3). The optimal configurations are illustrated in Fig. 10. It is noted that the optimal structure for the modified problem has a similar volume to the original problem, however the cross-sectional areas of the bars were significantly different. Bar (3), which in the original problem has no internal force and minimal area, became the one with higher normal force and largest area. In addition, the cross-sectional area of bar (4) in the original problem is about 45% larger

Table 4. Optimization results for the five-bar truss original problem.

	Scenario 1	Scenario 2
A_1 (10^{-4}m^2)	16.0416	16.1605
A_2 (10^{-4}m^2)	1.6444	1.6529
A_3 (10^{-4}m^2)	0.7854	0.7854
A_4 (10^{-4}m^2)	24.5040	24.5334
A_5 (10^{-4}m^2)	18.5233	18.6740
$f(\mathbf{x})$ (m^3)	0.0191	0.0191

than its optimal area in the second case. This fact emphasizes the importance of the correct definition of the boundary conditions, since optimal designs are highly dependent on this type of information.

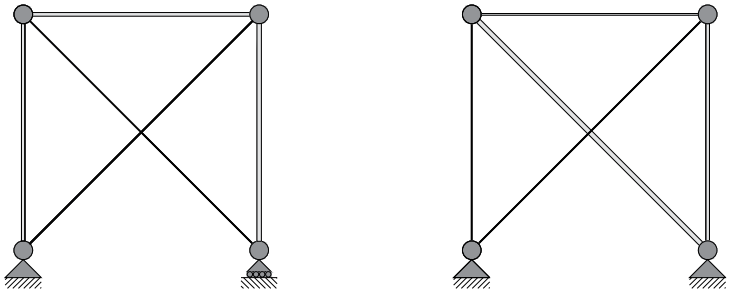

(a) Original. (b) Modified.

Figure 10. Optimal configurations of the five-bar truss problem.

5 Conclusions

This paper presented a comparison of optimal structural configurations obtained for two different constraint scenarios, considering elastic and inelastic buckling constraints, respectively, associated with yielding constraints. For each scenario, the effect of natural and essential boundary conditions was also studied. This investigation was performed for two plane trusses, one with two bars and another with five bars. A simple multistart scheme combined with sequential quadratic programming, was proposed for the optimization.

The first problem showed, as expected, that for bars under compression it is more useful to employ hollow cross sections with larger diameters and thinner. This points to the importance of imposing a limit on the ratio d/t to avoid very thin sections and, consequently, local instability of tube walls, or to apply more complex constraints to deal with local instability. Also, it was noted that scenario 2 gives more robust structures than scenario 1, in the cases were the bars are predominantly compressed. For structures with predominantly tensioned bars, the scenarios converge to results with very similar volumes. This indicates that scenario 2 is more restrictive with respect to buckling.

The second example showed that, for certain material properties, the optimal structures for each scenario can be the same, and that changes in the essential boundary conditions of the problem may lead to significant differences in optimal configurations, thus emphasizing the necessity of a proper definition of the boundary conditions of the structure.

Acknowledgements

The authors gratefully acknowledge the financial support from Scientific and Technological Research Support Foundation of Santa Catarina State (FAPESC), Coordination of Superior Level Staff Improvement (CAPES) and National Council for Scientific and Technological Development (CNPq, via grant 302489/2017-7).

References

[1] Luh, G.-C. & Lin, C.-Y., 2011. Optimal design of truss-structures using particle swarm optimization. *Computers & Structures*, vol. 89, n. 23-24, pp. 2221–2232.

[2] Stromberg, L. L., Beghini, A., Baker, W. F., & Paulino, G. H., 2012. Topology optimization for braced frames: Combining continuum and beam/column elements. *Engineering Structures*, vol. 37, pp. 106–124.

[3] Camp, C. V. & Huq, F., 2013. CO2 and cost optimization of reinforced concrete frames using a big bang-big crunch algorithm. *Engineering Structures*, vol. 48, pp. 363–372.

[4] Miguel, L. F. F., Lopez, R. H., & Miguel, L. F. F., 2013. Multimodal size, shape, and topology optimisation of truss structures using the Firefly algorithm. *Advances in Engineering Software*, vol. 56, pp. 23–37.

[5] Zegard, T. & Paulino, G. H., 2016. Bridging topology optimization and additive manufacturing. *Structural and Multidisciplinary Optimization*, vol. 53, n. 1, pp. 175–192.

[6] Farshchin, M., Camp, C. V., & Maniat, M., 2016. Optimal design of truss structures for size and shape with frequency constraints using a collaborative optimization strategy. *Expert Systems with Applications*, vol. 66, pp. 203–218.

[7] Tapao, A. & Cheerarot, R., 2017. Optimal parameters and performance of artificial bee colony algorithm for minimum cost design of reinforced concrete frames. *Engineering Structures*, vol. 151, pp. 802–820.

[8] Gomes, W. J. S., Beck, A. T., Lopez, R. H., & Miguel, L. F. F., 2018. A probabilistic metric for comparing metaheuristic optimization algorithms. *Structural Safety*, vol. 70, pp. 59–70.

[9] Tejani, G. G., Savsani, V. J., Bureerat, S., Patel, V. K., & Savsani, P., 2019. Topology optimization of truss subjected to static and dynamic constraints by integrating simulated annealing into passing vehicle search algorithms. *Engineering with Computers*, vol. 35, n. 2, pp. 499–517.

[10] Pezeshk, S., Camp, C. V., & Chen, D., 2000. Design of nonlinear framed structures using genetic optimization. *Journal of structural engineering*, vol. 126, n. 3, pp. 382–388.

[11] Suleman, A. & Sedaghati, R., 2005. Benchmark case studies in optimization of geometrically nonlinear structures. *Structural and Multidisciplinary Optimization*, vol. 30, n. 4, pp. 273–296.

[12] Lanes, R. M., Greco, M., & Guerra, M. B. B. F., 2019. Strut-and-tie models for linear and nonlinear behavior of concrete based on topological evolutionary structure optimization (ESO). *IBRACON structures and materials journal*, vol. 12, n. 1, pp. 87–100.

[13] Buhl, T., Pedersen, C. B. W., & Sigmund, O., 2000. Stiffness design of geometrically nonlinear structures using topology optimization. *Structural and Multidisciplinary Optimization*, vol. 19, n. 2, pp. 93–104.

[14] Jung, D. & Gea, H. C., 2004. Topology optimization of nonlinear structures. *Finite Elements in Analysis and Design*, vol. 40, n. 11, pp. 1417–1427.

[15] Kemmler, R., Lipka, A., & Ramm, E., 2005. Large deformations and stability in topology optimization. *Structural and Multidisciplinary Optimization*, vol. 30, n. 6, pp. 459–476.

[16] Klarbring, A. & Strömberg, N., 2013. Topology optimization of hyperelastic bodies including non-zero prescribed displacements. *Structural and Multidisciplinary Optimization*, vol. 47, n. 1, pp. 37–48.

[17] Zhang, X., Ramos Jr., A. S., & Paulino, G. H., 2017. Material nonlinear topology optimization using the ground structure method with a discrete filtering scheme. *Structural and Multidisciplinary Optimization*, vol. 55, n. 6, pp. 2045–2072.

[18] Nocedal, J. & Wright, S. J., 1999. *Numerical Optimization*. Springer-Verlag, New York, EUA.

[19] Arora, J. S., 2004. *Introduction to Optimum Design*. Elsevier Academic Pres, San Diego, CA, EUA, 2nd edition.

[20] Torii, A. J., Lopez, R. H., & Miguel, L. F. F., 2015. Modeling of global and local stability in optimization of truss-like structures using frame elements. *Structural and Multidisciplinary Optimization*, vol. 51, n. 6, pp. 1187–1198.

[21] Juliani, M. A. & Gomes, W. J. S., 2017-a. Influence of limit states on the optimization of reinforced concrete beams. *VI International Symposium on Solid Mechanics (MecSol)*, vol. , pp. 943–954.

[22] Juliani, M. A. & Gomes, W. J. S., 2017-b. Influence of limit states on the optimization of reinforced concrete plane frames. *XXXVIII Iberian Latin-American Congress on Computational Methods in Engineering (CILAMCE)*, vol. .

[23] Petrović, N., Marjanović, N., Kostić, N., Blagojević, M., Matejić, M., & Troha, S., 2018. Effects of introducing dynamic constraints for buckling to truss sizing optimization problems. *FME transactions*, vol. 46, n. 1, pp. 117–123.

[24] Galante, M., 1996. Genetic algorithms as an approach to optimize real-world trusses. *International Journal for Numerical Methods in Engineering*, vol. 39, pp. 361–382.

[25] Guo, X., Cheng, G., & Yamazaki, K., 2001. A new approach for the solution of singular optima in truss topology optimization with stress and local buckling constraints. *Structural and Multidisciplinary Optimization*, vol. 22, n. 5, pp. 364–373.

[26] Pedersen, N. L. & Nielsen, A. K., 2003. Optimization of practical trusses with constraints on eigenfrequencies, displacements, stresses, and buckling. *Structural and Multidisciplinary Optimization*, vol. 25, n. 5-6, pp. 436–445.

[27] Guo, X., Cheng, G. D., & Olhoff, N., 2005. Optimum design of truss topology under buckling constraints. *Structural and Multidisciplinary Optimization*, vol. 30, n. 3, pp. 169–180.

[28] Mela, K., 2014. Resolving issues with member buckling in truss topology optimization using a mixed variable approach. *Structural and Multidisciplinary Optimization*, vol. 50, n. 6, pp. 1037–1049.

[29] Beck, A. T. & Gomes, W. J. S., 2012. A comparison of deterministic, reliability-based and risk-based structural optimization under uncertainty. *Probabilistic Engineering Mechanics*, vol. 28, pp. 18–29.

[30] Aoues, Y. & Chateauneuf, A., 2010. Benchmark study of numerical methods for reliability-based design optimization. *Structural and Multidisciplinary Optimization*, vol. 41, n. 2, pp. 277–294.

[31] MathWorks, 2017. *MATLAB: Primer*. Natick, MA, EUA.

[32] Ziemian, R. D. & McGuire, W., 2007. *Tutorial for MASTAN2: version 3.0*. John Wiley & Sons.

[33] Madah, H. & Amir, O., 2017. Truss optimization with buckling considerations using geometrically nonlinear beam modeling. *Computers & Structures*, vol. 192, pp. 233–247.

[34] McGuire, W., Gallagher, R. H., & Ziemian, R. D., 2014. *Matrix Structural Analysis*. 2nd edition.

[35] Martí, R., 2003. *Multi-Start Methods. In: Glover F., Kochenberger G.A. (eds) Handbook of Metaheuristics. International Series in Operations Research & Management Science*, volume 57. Springer, Boston, MA, EUA.